catalysts

MDPI

Article

Application of Recombinant [NiFe]-Hydrogenase for Sustainable Coenzyme Regeneration

Renata Vičević [1], Zrinka Karačić [2], Maja Milunić [1], Anita Šalić [1,*], Ana Jurinjak Tušek [3] and Bruno Zelić [1,4]

[1] Faculty of Chemical Engineering and Technology, University of Zagreb, Trg Marka Marulića 19, HR-10000 Zagreb, Croatia; rvicevic@fkit.unizg.hr (R.V.); mmilunic@fkit.hr (M.M.); bzelic@fkit.unizg.hr (B.Z.)
[2] Ruđer Bošković Institute, Bijenička cesta 54, HR-10000 Zagreb, Croatia; zkaracic@irb.hr
[3] Faculty of Food Technology and Biotechnology, University of Zagreb, Pierottijeva 6, HR-10000 Zagreb, Croatia; ana.tusek.jurinjak@pbf.unizg.hr
[4] Department of Packaging, Recycling and Environmental Protection, University North, Trg dr. Žarka Dolinara 1, HR-48000 Koprivnica, Croatia
* Correspondence: asalic@fkit.unizg.hr

Abstract

Hydrogenases are key enzymes in microbial energy metabolism, catalyzing the reversible conversion between molecular hydrogen and protons. Among them, [NiFe]-hydrogenases are particularly attractive for biocatalytic applications due to the oxygen tolerance of several members of this class and their ability to couple hydrogen oxidation with redox cofactor regeneration. In this study, a recombinant soluble [NiFe]-hydrogenase from *Cupriavidus necator* H16 was successfully expressed in *Escherichia coli* BL21 (DE3), purified, and characterised with a focus on its applicability for NAD^+ regeneration. Unlike previous studies that primarily used native *C. necator* extracts or complex maturation systems, this work provides the first quantitative demonstration that an aerobically purified recombinant soluble [NiFe]-hydrogenase expressed in *E. coli* can function effectively as an NAD^+ regeneration catalyst and operate within multi-enzymatic cascade reactions under application-relevant conditions. The crude recombinant enzyme displayed a volumetric activity of 0.273 ± 0.024 U/mL and a specific activity of 0.018 ± 0.002 U/mg_{cells} in the hydrogen oxidation assay, while purification yielded a specific activity of 0.114 ± 0.001 U/mg with an overall recovery of 79.2%. The enzyme exhibited an optimal temperature of 35 °C and a pH optimum of 7.00. Thermal stability analysis revealed rapid deactivation at 40 °C ($k_d = 0.4186 \pm 0.0788$ h^{-1}, $t_{1/2} \approx 1.7$ h) and substantially slower deactivation at 4 °C ($k_d = 0.1141 \pm 0.0139$ h^{-1}, $t_{1/2} \approx 6.1$ h). Batch NADH oxidation experiments confirmed efficient cofactor turnover and high specificity towards NADH over NADPH. Finally, integration of the hydrogenase into a one-pot two-enzyme glucose oxidation system demonstrated its capacity for *in situ* NAD^+ regeneration, although the reaction stopped after approximately 5 min due to acidification from gluconic acid formation, highlighting pH control as a key requirement for future process optimization.

Keywords: NAD^+ regeneration; *E. coli* BL21 (DE3); [NiFe]-hydrogenase; enzyme purification

Check for updates

Received: 19 November 2025
Revised: 18 December 2025
Accepted: 20 December 2025
Published: 23 December 2025

Copyright: © 2025 by the authors. Licensee MDPI, Basel, Switzerland. This article is an open access article distributed under the terms and conditions of the Creative Commons Attribution (CC BY) license.

1. Introduction

Hydrogenases are key catalysts in microbial energy metabolism. They mediate the reversible interconversion of molecular hydrogen (H_2) and protons. Due to this fundamental activity, they are increasingly explored as versatile biocatalysts in various biotechnological applications. They are classified into three types: [FeFe]-hydrogenase, [NiFe]-hydrogenase

and [Fe]-hydrogenase, based on the metal composition of their active site [1]. Among them, [NiFe]-hydrogenases are the most widespread and occur in archaea, bacteria and some eukaryotes [2]. They typically have a heterodimeric structure. The catalytic large subunit contains the NiFe active site, while the small harbouring [4Fe4S] clusters that mediate electron transfer [1]. A distinguishing feature of several [NiFe]-hydrogenases is their tolerance to oxygen [3]. While many hydrogenases are irreversibly inactivated in the presence of O_2, some [NiFe]-hydrogenases retain substantial activity under oxidizing conditions. This property makes them particularly attractive for applied biocatalytic systems [4–7]. Despite their potential, hydrogenases are complex metalloenzymes that require elaborate maturation pathways involving multiple accessory proteins [8]. Their low abundance in native hosts and the difficulty of isolating active forms have therefore motivated the use of genetically engineered *Escherichia coli* for heterologous expression. *E. coli* BL21 (DE3), with its rapid growth and efficient protein production machinery, is the preferred host. It enables high-level expression, often up to 50% of total cellular protein [9–13], followed by purification via straightforward affinity-based methods [14].

As in the native host, a major biochemical challenge in the heterologous expression of [NiFe]-hydrogenases in *E. coli* is the requirement for a complex maturation process. Assembly of the catalytic NiFe centre depends on the Hyp maturation machinery (HypA-F). This system orchestrates metal trafficking, cyanation and carbonylation of the Fe site, formation of Fe-S clusters, and proteolytic processing of the large subunit. Because *E. coli* does not naturally provide this complete maturation pathway in sufficient amounts for the production of oxygen-tolerant [NiFe]-hydrogenases, co-expression of the Hyp gene cluster is essential. Furthermore, proper metal loading can be limiting in heterologous hosts. Supplementation of the culture medium with Ni^{2+} and Fe^{3+} ions necessary to achieve full catalytic activity [15,16].

In addition to maturation requirements, the physiological state of the expression host strongly affects hydrogenase functionality. Environmental stresses such as elevated NaCl concentrations [17,18], oxidative stress, or unintended oxygen exposure during expression can interfere with Fe-S cluster stability. They may also disrupt metal incorporation, or alter the redox environment required for proper folding and cofactor assembly [19–21]. These factors can result in misfolded or partially matured enzyme with reduced activity. Therefore, optimizing ionic strength, aeration, and redox conditions during expression is critical to maximizing the yield of active recombinant [NiFe]-hydrogenase.

One of the most prominent and well-studied members of the [NiFe]-hydrogenase family is the soluble hydrogenase (SH) from *Cupriavidus necator* H16. SH is a heterohexamer composed of the diaphorase subunits HoxF and HoxU, the hydrogenase subunits HoxY and HoxH, and a HoxI dimer that participates in NAD(P)H activation (Figure 1). The gene cluster coding for SH, *hoxFUYHWI*, contains a non-structural protein, the hoxW maturase, which is necessary for HoxH maturation. In general, the production of [NiFe]-hydrogenases is a complex maturation process requiring several auxiliary enzymes. For heterologous expression of SH in *E. coli*, an additional plasmid with the *hypABCDEFX* gene cluster has been used to obtain active hydrogenase [3,22]. The mechanism of oxygen-tolerance of this extraordinary enzyme is still unclear.

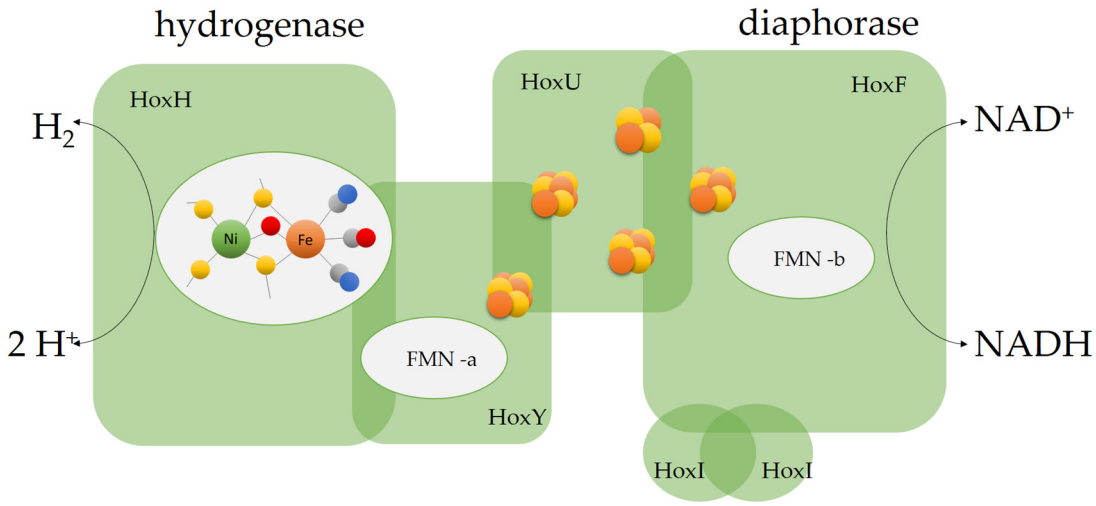

Figure 1. A schematic representation of soluble [NiFe]-hydrogenase from *C. necator* H16. HoxFU represents the diaphorase and HoxHY the hydrogenase moiety of the enzyme. The locations of FeS clusters and cofactor binding sites are indicated approximately. The HoxH subunit contains the binuclear active site where the hydrogenase reaction takes place.

Beyond hydrogen turnover [23], an important functional advantage of many [NiFe]-hydrogenases, including SH, is their ability to couple H_2 oxidation directly to the regeneration of essential redox cofactors such as NAD^+/NADH [7]. Efficient cofactor recycling is a central challenge in biocatalytic synthesis. In such systems oxidoreductases require continuous cofactor turnover to maintain high reaction rates [24]. Conventional regeneration systems, such as NADH oxidase (NOX), rely on molecular oxygen as the terminal electron acceptor. However, poor oxygen solubility and slow mass transfer severely limit scalability and process control. These limitations highlight the need for robust, oxygen-independent regeneration technologies [25–29].

Hydrogenases provide a compelling solution to this challenge [7,30,31]. By using H_2 as a clean and abundant electron donor, they enable NAD^+ regeneration under anaerobic or microaerobic conditions without dependence on oxygen. This capability offers improved efficiency, scalability, and integration into closed bioprocesses. Consequently, the application of hydrogenases in cofactor regeneration represents an attractive strategy for advancing sustainable biocatalytic platforms. Unlike most hydrogenases, SH is oxygen-tolerant and maintains catalytic activity under ambient O_2 levels [32]. This property enables its use in O_2-dependent multi-enzymatic cascades and biotransformations [4–6].

Over the last decade, the Vincent group at the University of Oxford has produced an extensive and influential body of work on [NiFe]-hydrogenases, significantly advancing their fundamental understanding and technological relevance [33–38]. Their studies have elucidated key aspects of hydrogenase catalysis, including oxygen tolerance, redox behaviour, electron-transfer kinetics, and catalytic bias, primarily through electrochemical and spectroscopic approaches. Importantly, this work has demonstrated the feasibility of coupling H_2 oxidation by [NiFe]-hydrogenases to NAD^+/NADH recycling, establishing hydrogenases as efficient redox modules for cofactor regeneration. In parallel, efforts have been directed towards the expression, engineering, and functional tuning of *E. coli* hydrogenases, enabling their integration into biotechnological and semi-artificial catalytic systems. Despite these advances, relatively limited attention has been given to the practical production, purification, and quantitative kinetic characterisation of recombinant, oxygen-tolerant soluble hydrogenases expressed in *E. coli* under application-relevant conditions, particularly regarding their direct use as stand-alone NAD^+ regeneration catalysts.

This study focuses on the recombinant production and characterization of the soluble [NiFe]-hydrogenase from *C. necator* H16 in *E. coli* BL21 (DE3). By examining its catalytic properties, stability, and ability to drive $NAD(P)^+$ regeneration, this work provides insight into the feasibility of using recombinant [NiFe]-hydrogenases as biocatalysts for cofactor regeneration. As a final step, [NiFe]-hydrogenase was coupled with glucose dehydrogenase in the glucose oxidation reaction, serving as a model system for further studies on biohydrogen production.

2. Results and Discussion

Ultrasonic treatment is most commonly used to release recombinant proteins from *E. coli*, as it does not require sophisticated equipment and is easy to handle [39]. Therefore, *E. coli* BL21 (DE3) cells expressing the [NiFe]-hydrogenase were lysed under optimized sonication conditions (Appendix A Table A1, Figures A1–A3). This procedure yielded in a volumetric activity of V.A. = 0.273 ± 0.024 U/mL and a specific activity of S.A. = 0.018 ± 0.002 $U/mg_{cells.}$ When normalized to total protein, the specific activity was, S.A. 0.341 ± 0.070 $U/mg_{protein}$. The observed activities demonstrate good performance while also revealing clear opportunities for further optimization. Al-Shameri et al. [7] reported a specific activity of 0.22 U/mg at 1 mM NADH, which is in a similar range to our results when differences in assay conditions and enzyme preparation are taken into consideration. Fan et al. [40] achieved a specific activity of 0.5 U/mg for a heterologously expressed regulatory [NiFe]-hydrogenase from *C. necator* in *E. coli*. They also reported high volumetric yields of catalytically active enzyme (~80 mg/L), corresponding to a 160-fold improvement relative to the native host. Likewise, Schiffels et al. [3] reported activities up to 7.2 ± 1.15 U/mg_{cells} for other [NiFe]-hydrogenases. Together, these literature values highlight the well-established variability in hydrogenase performance across expression hosts, assay conditions, and enzyme classes. At the same time, they illustrate that the system described here provides a solid functional baseline that can be further enhanced through optimization of expression, maturation, and assay parameters.

2.1. Characterization of the Crude Recombinant [NiFe]-Hydrogenase from E. coli BL21 (DE3)

The crude extract obtained by ultrasonic treatment was used as the starting material for initial [NiFe]-hydrogenase characterisation. At this stage, a preliminary assessment of [NiFe]-hydrogenase activity was performed before further purification steps to obtain more information about the intrinsic properties of the enzyme. Determining the optimal pH and temperature is essential, as many enzymes exhibit high catalytic activity only within narrow ranges. Outside these limits, conformational changes may occur, leading to partial or complete loss of catalytic activity. Furthermore, defining these parameters is crucial for establishing suitable reaction conditions for future applications in biohydrogen production.

pH strongly influences enzyme conformation, stability and catalytic efficiency [41]. Outside the optimal pH range, structural changes may occur at the enzyme active site or in the substrate. These changes reduce substrate binding and lead to a decrease in overall activity [42,43]. Both pH and temperature are fundamental parameters that determine catalytic performance. They strongly affect reaction kinetics, enzyme conformation, structural stability, and overall activity [42,44]. Increasing the temperature up to an optimum increases the kinetic energy of the molecules, accelerates enzyme–substrate collisions, and increases activity. However, exceeding the optimal temperature results in enzyme denaturation, loss of secondary and tertiary structure, and reduced catalytic activity [45]. Stability tests were therefore carried out to determine the conditions under which the enzyme retains its functionality over an extended period. This information is essential for optimizing process

conditions and for defining appropriate storage strategies that preserve enzyme activity for use in biotechnological processes.

The dependence of relative activity on pH is shown in Figure 2a. In this study, the highest activity for the hydrogen reduction reaction was observed at pH 7.00, indicating that the enzyme operates most efficiently under neutral conditions. The protonation state of amino acid residues in the active site plays a key role in catalytic efficiency, and neutral pH appears to provide the most favourable environment for substrate binding and electron transfer [46–48]. In addition, the stability of NADH at λ = 340 nm is highest near neutral pH, ensuring reliable and reproducible measurements of enzymatic activity [49]. The pH optimum determined in this work is consistent with literature reports. Kim et al. [11] found that recombinant [NiFe]-hydrogenase expressed in *E. coli* exhibited maximal hydrogen production at pH 6.80, which closely agrees with the pH 7.00 optimum observed here. Their study also highlighted the enzyme's ability to function in the presence of oxygen, underscoring its potential for practical biohydrogen production. Reported pH optima across different studies range from 6.3 to 8.4 [30,50–52]. These variations likely reflect structural differences between hydrogenases from different organisms or recombinant systems, including changes in the protonation state of amino acids near the active site that can subtly influence catalytic behaviour.

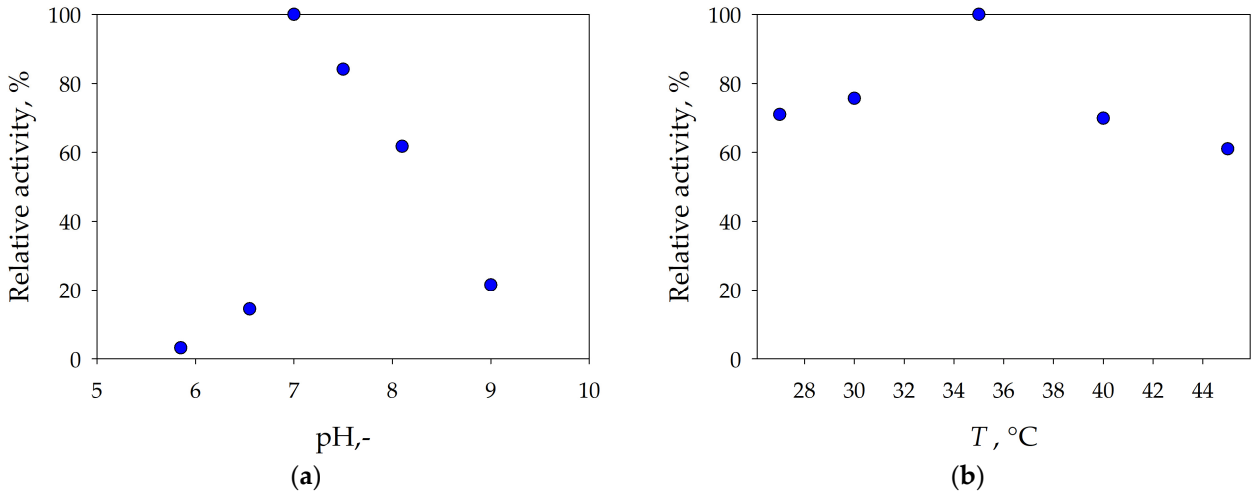

Figure 2. Optimal pH (**a**) and temperature (**b**) conditions for the activity of recombinant [NiFe]-hydrogenase.

These discrepancies emphasize the importance of experimentally determining the optimal conditions for each enzyme variant. In experiments with the crude extract, the maximum volumetric activity was V.A. = 0.130 ± 0.001 U/mL for hydrogen reduction. Such behaviour has been reported for [NiFe]-hydrogenases, particularly those that are oxygen tolerant [53]. In contrast, [FeFe]-hydrogenases generally show a greater preference for hydrogen production, but at the expense of increased oxygen sensitivity [54].

As previously mentioned, the influence of temperature on reaction rate is one of the most important aspects in the characterisation of enzymes, as it directly determines the conditions under which the enzyme exhibits maximal catalytic activity. In this study, the temperature optimum of the recombinant [NiFe]-hydrogenase was evaluated over a range from 27 to 45 °C. The results shown in Figure 2b clearly indicate that the enzyme reaches its maximum activity at 35 °C. These findings are consistent with literature data, which report optimal temperatures of 33 °C [55] and 35 °C [23] for the soluble [NiFe]-hydrogenase (SH) from *C. necator* H16. In the case of recombinant enzymes, incomplete maturation can also contribute to reduced catalytic activity [56]. Because the recombinant [NiFe]-hydrogenase

catalyses reactions involved in coenzyme regeneration, achieving and maintaining the optimal temperature is critical to ensure efficient turnover. When the reaction temperature is below the optimum, enzymatic reaction rates decrease, resulting in lower overall activity. In contrast, temperatures above the optimal range can lead to enzyme denaturation, loss of tertiary structure, and complete loss of catalytic function [57].

The stability of the recombinant [NiFe]-hydrogenase was therefore evaluated at different temperatures (T = 4 °C and T = 40 °C) to assess its robustness during storage and processing (Figure 3). The measured enzyme activities were converted to relative activities to facilitate interpretation and comparison.

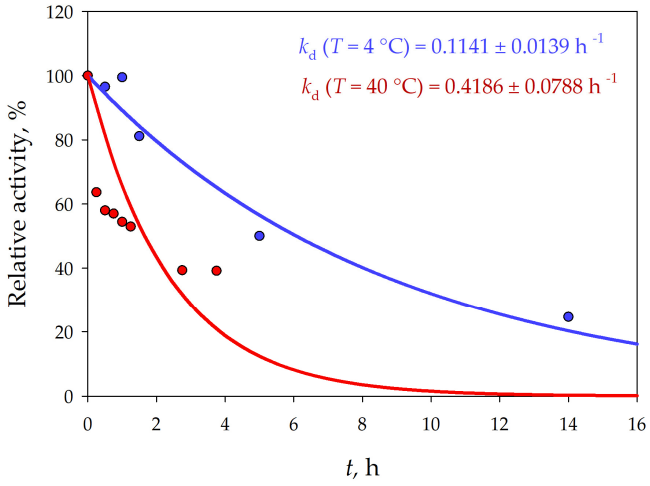

Figure 3. The influence of temperature on the stability of [NiFe]-hydrogenase with deactivation constants, k_d (● T = 40 °C, ● T = 4 °C, – mathematical model).

From the experimental data obtained, the deactivation constants of the enzyme were determined to be k_d = 0.1141 ± 0.0139 1/h at T = 4 °C, and k_d = 0.4186 ± 0.0788 1/h at T = 40 °C. These results clearly indicate that the enzyme is significantly more stable at lower temperatures. The deactivation constant at T = 40 °C is approximately 3.7-fold higher than that measured at T = 4 °C. It can therefore be concluded that low temperatures contribute to enzyme stabilization and help maintain catalytic activity over extended periods. In contrast, elevated temperatures markedly accelerate the loss of functionality, rendering the enzyme unsuitable for processes that require higher operating temperatures. Consistent with these findings, Chowdhury et al. [58] reported that hydrogenase activity from soil samples was irreversibly lost at temperatures slightly above 30 °C, demonstrating the high sensitivity of hydrogenase to thermal degradation. Keefe et al. [59] likewise observed that NAD^+-dependent hydrogenases retained high activity at low temperatures without significant deactivation over prolonged periods. Overall, the literature [60,61] confirms the general tendency of hydrogenases to exhibit high stability at 4 °C, whereas rapid deactivation occurs at elevated temperatures (≥30–40 °C).

2.2. Isolation of the Recombinant [NiFe]-Hydrogenase from Crude Extract

Purification is required to increase the specific activity of an enzyme [60] and to remove impurities that may interfere with activity assays and protein quantification. While some applications require a high degree of enzyme purity, others can tolerate lower purity levels, allowing the use of crude enzyme preparations [60]. Purified enzymes often exhibit higher stability, primarily because contaminating components that promote degradation are removed [62]. However, increasing the degree of purity also raises the overall cost of enzyme production [60]. After purification, the success of the process must be evaluated. Several analytical methods are available for this purpose, with SDS-PAGE being the most

commonly used. This technique separates proteins according to their molecular size and can also be used to determine their relative molecular weights [63]. In crude extracts, SDS-PAGE typically reveals numerous overlapping protein bands, which complicates identification of the target enzyme. After purification, this complexity is reduced, and most proteins appear as distinct bands on the gel [64]. [NiFe]-hydrogenases can be readily identified by the presence of five characteristic bands corresponding to the large and small subunits of the enzyme complex [65].

After cultivation of the transformed cells and optimisation of [NiFe]-hydrogenase extraction and characterisation, the enzyme was purified. The success of the purification process was verified by SDS-PAGE analysis (Figure 4). Bands corresponding to the molecular masses of the protein subunits HoxF (67.8 kDa), HoxH (54.9 kDa), HoxU (26.6 kDa), HoxY (22.9 kDa) and HoxI (18.6 kDa) were clearly visible. This band pattern is consistent with literature data describing the subunit composition of [NiFe]-hydrogenase [65].

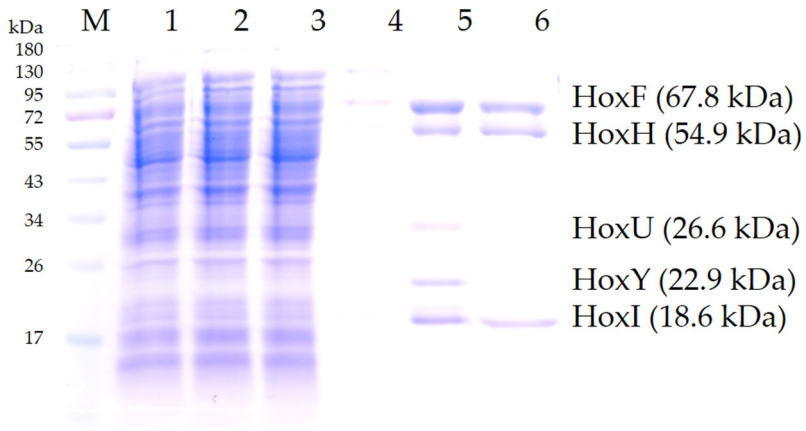

Figure 4. Purification of SH from *E. coli* on a StrepTrapXT column, shown as fractions on a 12% gel. Lanes contain: M–PageRuler Prestained Protein Ladder (Thermo Fischer Scientific), 1—cleared cell lysate, 2—flow-through, 3—wash fraction 1, 4—wash fraction 3, 5—elution fraction 1, 6—elution fraction 2. Additional SDS–PAGE lanes showing samples before and after induction were not included, as they did not provide informative evidence of overexpression; the recombinant [NiFe]-hydrogenase does not produce a clearly distinguishable overexpressed band under these conditions.

As previously mentioned, *C. necator* H16 contains a soluble cytoplasmic [NiFe]-hydrogenase that establishes a direct link between the NAD^+/NADH redox couple and hydrogen metabolism [66]. This soluble [NiFe]-hydrogenase is encoded by the *hoxFUYHWI* operon. The HoxFU subunits are responsible for electron transfer between NAD^+/NADH and the catalytic centre, where HoxYH constitutes the hydrogenase module where hydrogen conversion occurs. The HoxI subunit stabilises the overall enzyme structure, and HoxW acts as a maturation protease required for the final activation of the catalytic HoxH subunit. The HoxH subunit is particularly crucial, as it contains the active site where molecular hydrogen binds and is activated [65,67]. Without proper expression, processing, and assembly of these subunits, the enzyme would remain non-functional and unable to catalyse hydrogen conversion reactions [22].

Before purification, the [NiFe]-hydrogenase volumetric activity was determined via the NADH oxidation assay and was V.A. = 0.130 ± 0.001 U/mL (S.A. = 0.144 ± 0.001 U/mg). After purification, the volumetric activity decreased to V.A. = 0.034 ± 0.001 U/mL (S.A. = 0.114 ± 0.001 U/mg). Although purification increased sample purity, it resulted in a slight reduction in specific activity of approximately 21%, corresponding to an overall activity recovery of 79.2%. This decrease may be attributed to partial enzyme loss or inactivation during purification. Additionally, the removal of endogenous enzymes, such

as NADH oxidase, may contribute to the observed effect. Such enzymes can participate in NADH oxidation in crude extracts and artificially inflate apparent activity values [68].

Because the yield of purified [NiFe]-hydrogenase was relatively low (approximately 1 µg per 10 mL of *E. coli* BL21 (DE3) crude extract), no further characterization of the purified [NiFe]-hydrogenase was performed in this study.

2.3. NAD(P)H Oxidation in a Batch Reactor

Prior to coenzyme regeneration, coenzyme stability was evaluated. Both NADH and NADPH are susceptible to chemical degradation in aqueous solutions, particularly under unfavourable pH conditions or at elevated temperatures [49]. This instability presents a significant limitation for their application in biotechnological processes, as degraded cofactors can no longer efficiently serve as electron donors in reduction reactions. Although NADH and NADPH are structurally similar, differences in their stability can influence their suitability as reaction substrates. Therefore, assessing coenzyme stability across a range of pH values and elevated temperatures is essential. This evaluation enables optimization of reaction conditions, minimizes cofactor loss, and defines the time window over which hydrogen production can proceed efficiently. Coenzyme stability was assessed over a pH range of 4.25 to 8.00 at T = 35 °C, which corresponds to the optimal temperature determined for the recombinant [NiFe]-hydrogenase. The results are shown in Figure A4. Degradation constants (k) for NADH and NADPH were calculated at different pH values (Table A2). The data indicate that both coenzymes are significantly more stable under neutral conditions, whereas acidic pH values markedly accelerate their degradation.

Finally, NAD(P)H oxidation experiments were conducted under previously determined optimal conditions (pH 7.00 and T = 35 °C) in a batch reactor (V = 50 mL). Three different catalysts were evaluated: crude extract from *E. coli* BL21 (DE3) cells expressing recombinant [NiFe]-hydrogenase, purified recombinant [NiFe]-hydrogenase and crude extract from *C. necator* H16 cells. The results of NADH oxidation are shown in Figure 5a, while those of NADPH oxidation are shown in Figure 5b.

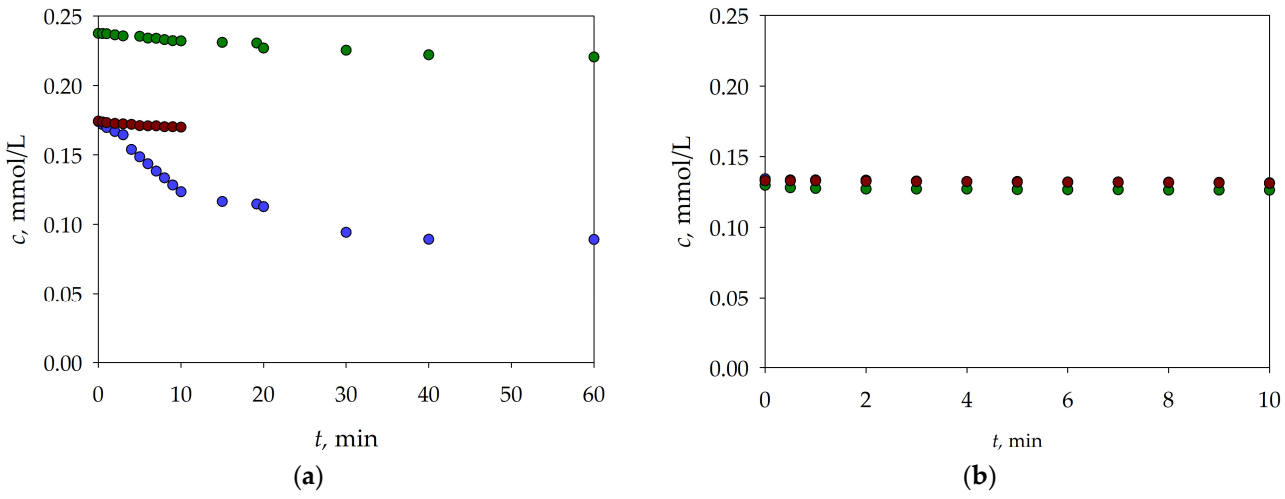

Figure 5. (**a**) NADH and (**b**) NADPH oxidation at pH 7.00 using: (●) crude extract from *E. coli* BL21 (DE3) cells with recombinant [NiFe]-hydrogenase, (●) purified recombinant [NiFe]-hydrogenase, (●) crude extract from *C. necator* H16 cells.

The results reveal pronounced differences in the temporal changes of coenzyme concentration catalysed by crude extracts and the purified enzyme (Figure 5a). Although identical enzyme concentrations were used in all experiments, the initial activities differed markedly. The crude recombinant *E. coli* extract exhibited the highest NADH consumption

(V.A. ≈ 0.00534 U/mL). The purified *E. coli* [NiFe]-hydrogenase showed lower but literature-consistent NADH oxidation (V.A. ≈ 0.00136 U/mL) [7]. In contrast, the crude *C. necator* H16 extract resulted in the smallest decrease in coenzyme concentration (V.A. ≈ 0.00140 U/mL). These results illustrate the strong influence of enzyme source and initial activity on NADH oxidation under the applied experimental conditions.

The results observed for the recombinant [NiFe]-hydrogenase expressed in *E. coli* BL21 (DE3) are not unexpected. The crude extract contains, in addition to the target [NiFe]-hydrogenase, other proteins and cellular components that may indirectly enhance reaction efficiency. Examples include NADH oxidase and other auxiliary enzymes [69]. Furthermore, crude extracts may contain components that act as enzyme stabilisers, protecting the hydrogenase from denaturation and activity loss [70]. However, the disadvantages of using crude extract should also be considered. The increased apparent coenzyme regeneration in the crude extract does not necessarily originate exclusively from [NiFe]-hydrogenase activity. Non-specific reactions involving other enzymes and metabolites present can also contribute. In particular, non-specific NADH consumption is problematic, as this coenzyme participates in numerous side reactions in addition to the desired process. This reduces selectivity and reproducibility. In contrast, purified enzymes are isolated from the cellular environment and lack protective molecules, which often leads to partial activity loss during purification [71]. Nevertheless, purified enzymes provide a more defined and specific catalytic system. Although their apparent activity may be lower, they offer a more reliable basis for the development of controlled and reproducible bioprocesses. The results in Figure 5a further show that the crude extract from *C. necator* H16 is less active than the crude extract containing recombinant [NiFe]-hydrogenase from *E. coli* BL21 (DE3). This indicates that the amount and availability of catalytically active enzyme in the wild-type strain are significantly lower than in the recombinant expression systems. Recombinant *E. coli* BL21 (DE3) is engineered to overexpress the target enzyme, resulting in higher intracellular concentrations of active hydrogenase in the crude extract. Both the crude extract and the purified enzyme were also tested for NADPH oxidation, and the results are shown in Figure 5b.

A direct comparison of Figure 5a,b demonstrates that the [NiFe]-hydrogenase exhibits strong specificity for NADH rather than NADPH. This finding is consistent with previous reports by Burgdorf et al. [65]. Overall, these results suggest that the use of crude extract from recombinant *E. coli* BL21 (DE3), as well as the purified recombinant enzyme, represents a more efficient strategy for process productivity than the use of the wild-type enzyme. In addition, substrate selection is crucial, as [NiFe]-hydrogenases clearly favour NADH as the electron donor.

Finally, glucose oxidation catalysed by GDH, combined with parallel coenzyme regeneration by [NiFe]-hydrogenase, was carried out as a one-pot, two enzyme system. The results of this coupled reaction are presented in Figure 6.

In light of the previously evaluated coenzyme stability, which demonstrated that both NADH and NADPH undergo rapid chemical degradation under acidic conditions and at elevated temperatures, the behaviour observed in the two-enzyme glucose oxidation system can be directly attributed to the loss of a stable environment required for sustained cofactor turnover. Although NADH is significantly more stable at neutral pH, the rapid formation of gluconic acid during GDH-catalysed glucose oxidation causes a pronounced pH drop to 3.52 within the first five minutes of the reaction. This shift pushes the system into a regime in which both the hydrogenase and the coenzyme lose functional stability [72]. The time-course profiles obtained using crude *E. coli* extract, crude *C. necator* extract, and purified SH from *E. coli* all exhibit the same behaviour. An initial phase of efficient NAD^+ recycling catalysed by SH is followed by a complete stop of NADH oxidation and product

formation once the pH falls outside the operational window of the biocatalysts. Under these acidic conditions, GDH becomes inactive, and NADH degradation accelerates. As a result, the hydrogenase is no longer able to sustain a continuous regeneration loop. The slightly faster initial NADH turnover observed with the purified SH indicates that the hydrogenase itself is capable of supporting efficient cofactor regeneration under suitable conditions. However, in this system, the reaction medium rather than the enzyme becomes the limiting factor. These findings highlight the critical importance of effective pH control in future system designs. Without maintaining near-neutral pH values, whether through increased buffer capacity, implementation of pH-stat control, or *in situ* neutralisation strategies, the hydrogenase cannot be utilised to its full potential as a sustainable NAD^+ regeneration catalyst. This limitation is consistent with broader observations from the NAD(P)H oxidation experiments (Figure 5a,b). While the recombinant [NiFe]-hydrogenase expressed in *E. coli* exhibits strong activity towards NADH, its performance is highly dependent on the physicochemical stability of the coenzyme in the reaction environment. To overcome these limitations and improve overall process performance, the application of microreactor technology represents a promising approach. By shifting from batch to continuous operation, product inhibition can be avoided through continuous removal of reaction products. In addition, improved mixing, and enhanced heat and mass transfer in microreactors can increase reaction rates and reduce reaction time [73–76].

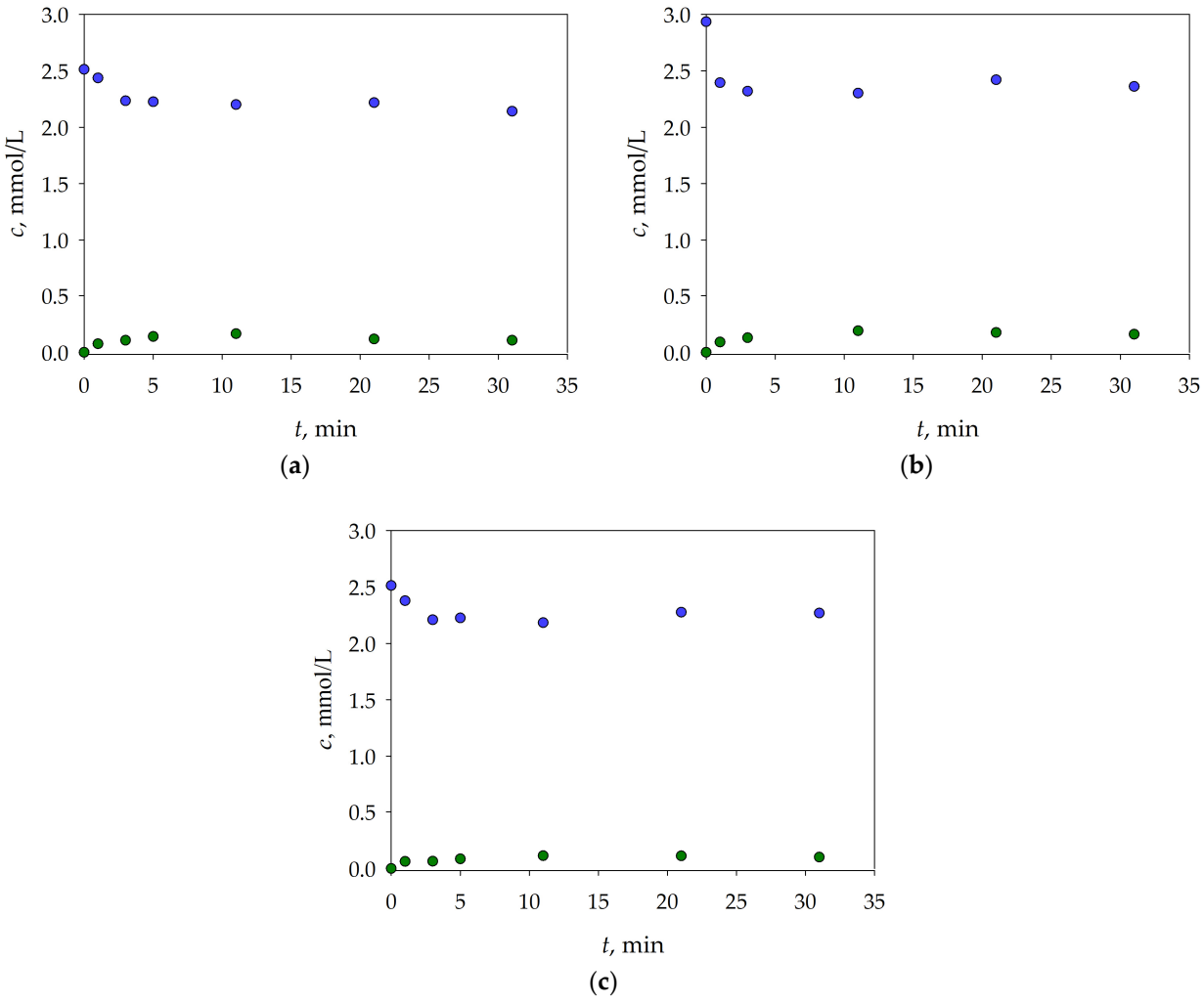

Figure 6. Oxidation of the glucose (●) in the presence of GDH and (**a**) crude extract from *E. coli* BL21 (DE3) cells with recombinant [NiFe]-hydrogenase (**b**) purified recombinant [NiFe]-hydrogenase (**c**) crude extract from *C. necator* H16 cells (NADH (●)).

3. Materials and Methods

3.1. Chemicals

Acetonitrile, acrylamide, ampicillin, biotin, Luria Bertani culture medium and ROTI Prep Plasmid MINI-XL plasmid isolation kit were purchased from Carl Roth (Karlsruhe, Germany). Dithiothreitol (DTT), nicotinamide adenine dinucleotide (NAD^+), nicotinamide adenine dinucleotide phosphate (NADPH) and nicotinamide adenine dinucleotide reduced (NADH) were procured from Thermo Fischer (Bremen, Germany). Bovine serum albumin (BSA), peptone, potassium acetate, β-mercaptoethanol and sodium dodecyl sulphate (SDS) were purchased from Sigma Aldrich (Saint Louis, MO, USA). Acetic acid was purchased from T.T.T. d.o.o. (Zagreb, Croatia). Ammonium peroxydisulfate (APS) was purchased from Alfa Aesar (Karlsruhe, Germany). Orthophosphoric acid was purchased from Merck (Darmstadt, Germany). *N*,*N*,*N*′,*N*′-tetramethylethylenediamine (TEMED) was purchased from TCI Europe N.V. (Haven, Belgium), while EDTA protease free inhibitor was purchased from Calbiochem (San Diego, CA, USA). Isopropyl β-D-1-thiogalactopyranoside (IPTG) was procured from Duchefa (Haarlem, The Netherlands), and Bromphenol Blue and glucose from Fischer Scientific (Merelbeke-Melle, Belgium). The glucose PAP test was purchased from Diagnostika (Sisak, Croatia). Coomassie Brilliant Blue G-250 was procured from Honeywell/Fluka (Seelze, Germany), and tris(hydroxymethyl)aminomethane was purchased from VWR Chemicals (Leuven, Belgium). Ethanol and hydrochloric acid were procured from Gram-Mol d.o.o. (Zagreb, Croatia). Potassium hydroxide was purchased from Acros Organics (Geel, Belgium). *E. coli* BL21 (DE3) was purchased from New Englands Biolabs (Ipswich, MA, USA). The plasmid for SH expression, pSH-hoxW (Figure 7), was ordered from Genscript (Rijswijk, The Netherlands). Plasmid pSU-A2-X, carrying 7 auxiliary enzymes for maturation of the *Cn* soluble [NiFe]-hydrogenase was a kind gift from Prof. Frank Sargent, Newcastle University, England [22].

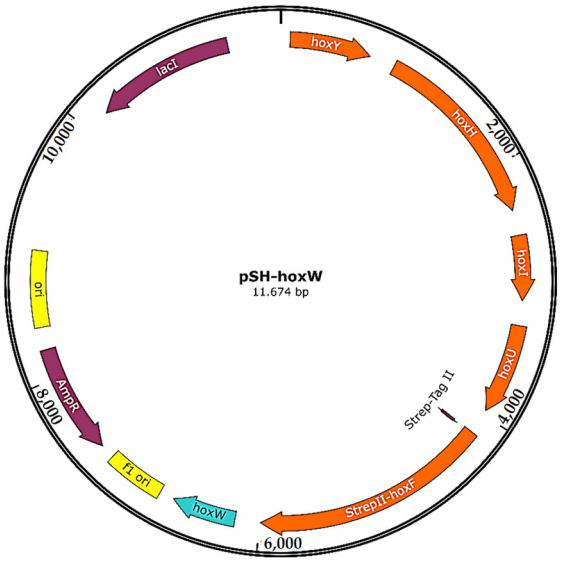

Figure 7. Map of plasmid pSH-hoxW.

3.2. Methods

3.2.1. Measurement of NADH and NADPH Concentration

The concentrations of NADH and NADPH were determined spectrophotometrically using a UV-VIS spectrophotometer (BK-D590, Biobase, Jinan, China) at a wavelength λ = 340 nm. All measurements were performed in triplicate. Quantification was based on calibration curves prepared with NADH and NADPH standards in the concentration range of 0.0375–0.3000 mmol/L.

3.2.2. Measurement of Glucose Concentration

Glucose concentration was determined spectrophotometrically using the glucose oxidase-4-aminoantipyrine (GOD-PAP) assay [77]. Briefly, 10 µL of the glucose sample was mixed with 1 mL of glucose PAP reagent and incubated for 20 min. Absorbance was then measured at λ = 500 nm using a spectrophotometer. Glucose concentrations were calculated from a calibration curve covering the range 0.17–5.55 mmol/L. All measurements were performed in triplicate, and results are presented as mean ± standard deviation.

3.2.3. Protein Concentration Measurements

Protein concentrations were determined using the linearized Bradford method, as described previously [78]. For each measurement, 500 µL of enzyme solution was mixed with 500 µL of Bradford reagent in a 1.0 cm path-length plastic cuvette. The mixture was incubated at T = 25 °C for 5 min, after which absorbance was measured at λ = 595 nm and λ = 450 nm using a UV-VIS spectrophotometer. To correct for background absorbance, the A_{595}/A_{450} ratio was used as the response variable. Protein concentrations were calculated by comparison with a calibration curve prepared using BSA standard in the concentration range 0–50 mg/L. Linear regression was applied, and enzyme samples were diluted appropriately when absorbance values fell outside the calibrated range. All measurements were performed in triplicate, and results are reported as mean ± standard deviation.

3.2.4. Determination of the Stability of the Coenzymes NADH and NADPH in Aqueous Solution

The stability of the coenzymes NADH and NADPH was evaluated in aqueous buffer systems. A 50 mmol/L potassium acetate buffer was used at pH values of 4.25, 4.60, and 5.00, while a 50 mmol/L Tris-HCl buffer was used at pH 6.00 and 7.00. Coenzymes were freshly prepared at an initial concentration of 0.2 mmol/L in the buffer and incubated at T = 35 °C. Absorbance at λ = 340 nm was recorded at regular intervals over a period of 30 min. Buffer blanks were measured in parallel to correct for background absorbance [79]. The coenzyme degradation constant (k) weas estimated from the experimental data using the software package Scientist (MicroMath® Scientist® for WindowsTM, Version 2.0, Salt Lake City, UT, USA), assuming first-order kinetics.

3.2.5. Measurement of [NiFe]-Hydrogenase Activity by Hydrogen Reduction Reaction

The [NiFe]-hydrogenase activity assay was based on spectrophotometric monitoring of NADH consumption, measured as a decrease in absorbance at λ = 340 nm. A solution containing 940 µL buffer (50 mmol/L Tris-HCl, pH 7.00), 10 µL 0.1 mol/L DTT and 10 µL 0.1 mol/L NADH was prepared. The hydrogen reduction reaction started by adding 40 µL of [NiFe]-hydrogenase. The decrease in absorbance, resulting from the oxidation of NADH to NAD^+ and the simultaneous formation of H_2, was monitored for 10 min at λ = 340 nm. Control reactions were performed in parallel, including (i) buffer without enzyme, and (ii) crude extract from non-transformed *E. coli* BL21 (DE3). No decrease in A_{340} was observed in control (i). The crude *E. coli* extract showed only a very low background rate of NADH oxidation, at least an order of magnitude below the activity measured for recombinant SH. Based on the data obtained, the volumetric and specific activities of the enzyme were calculated.

3.2.6. SDS-PAGE Analysis

SDS-PAGE was performed as described by Laemmli [80]. Protein samples were mixed with treatment buffer containing β-mercaptoethanol and incubated for 10 min at T = 96 °C. The samples were then separated on a 12% polyacrylamide gel. After electrophoresis, the gels were stained with Coomassie Brilliant Blue R-250.

3.2.7. Investigation of the Effects of pH and Temperature on the Activity and Storage Stability of Recombinant [NiFe]-Hydrogenase

Enzyme activity was assayed in the pH range 3.20–5.80 using 50 mmol/L potassium acetate buffer, and in the range 6.00–9.90 using 50 mmol/L Tris-HCl buffer. All pH-dependent activity measurements were performed at T = 25 °C. The influence of temperature on enzyme activity was assessed by measuring catalytic activity between T = 25 °C and T = 45 °C. Storage stability was investigated at two temperatures, T = 4 °C and T = 40 °C, over a period of 14 h. Samples were analysed spectrophotometrically at intervals of 0.5–1.0 h. The software package Scientist was used to estimate the [NiFe]-hydrogenase deactivation constant (k_d) from the data obtained, assuming first-order deactivation kinetics.

3.2.8. Expression of Recombinant [NiFe]-Hydrogenase in *E. coli* BL21 (DE3)

The expression plasmid pSH-hoxW used in this study (plasmid map created using SnapGene, Boston, MA, USA, Figure 7) is a recombinant vector designed for high-level expression of soluble [NiFe]-hydrogenase in *E. coli* BL21 (DE3), following previously reported successful approaches [3,7]. Five genes coding the structural subunits of the recombinant [NiFe]-hydrogenase, along with an additional gene encoding the HoxW maturase, were inserted into the pETDuet-1 vector, manufactured by GenScript (Rijswijk, The Netherlands). All genes contain their separate T7 promoter, lac operator, ribosome binding site, and T7 terminator, which ensures high inducible expression, proper transcription termination and stability of the synthesized mRNA. The order of the genes within the plasmid was changed from the natural order to achieve best protein expression, as described elsewhere [3]. However, for the oxygen-tolerant [NiFe]-hydrogenase to be properly produced, a set of maturases is also required. This was achieved by simultaneously transforming the bacteria with pSH-hoxW and pSU-A2-X plasmids [22].

Plasmid pSH-hoxW (with ampicillin resistance, Figure 7) was received as lyophilized DNA, reconstituted in sterile water and used as such for bacterial transformation. Plasmid pSU-A2-X (with kanamycin resistance) was obtained in the form of bacterial stock cultures (bacterial strain not specified) from Prof. Frank Sargent (Newcastle University). Fresh bacterial cultures were grown on solid LB medium with the addition of the antibiotic, followed by 10 mL overnight cultures prepared at T = 37 °C in liquid medium and used for plasmid isolation (ROTI®Prep Plasmid MINI-XL isolation kit). All cultures were grown under standard aerobic shaking conditions; no anaerobic or microaerobic measures were applied, consistent with the oxygen tolerance of the soluble SH.

The cell transformation was performed by heat shock, with 1 µL of each plasmid added to 50 µL of chemically competent *E. coli* BL21 (DE3) cells and the cells were inoculated on the double antibiotic plate. The colonies of transformants were inoculated into 50 mL of liquid medium the next day. The inoculated liquid culture media were incubated overnight on a shaker (PSE-T150A, Biolab, Berlin, Germany) at T = 37 °C.

To successfully express the recombinant [NiFe]-hydrogenase, metal cofactors had to be added to the medium [7]. In baffled flasks containing 1 L of TB (Terrific Broth) medium with antibiotics (final concentration 100 µg/mL), Ni(II) chloride (final concentration 100 µmol/L) and Fe(III) chloride (final concentration 100 µmol/L) were added along with 20 mL of overnight culture. The OD_{600} was monitored over time, and when it reached approximately 2.0, expression was induced with IPTG (final concentration 1 mmol/L). The cultures were then incubated at T = 18 °C and 120 rpm overnight. The cells were collected by centrifugation at 4000 rpm and T = 4 °C (EBA 8, Hettich Zentrifugen, Kirchlengern, Germany), and the pellets were frozen at T = –80 °C until use (Arctico ULTF 80®, Salisbury, UK).

3.2.9. Ultrasonic Treatment of *E. coli* BL21 (DE3) Cells

Frozen *E. coli* BL21 (DE3) cells were thawed at room temperature (T = 25 °C) and resuspended in 50 mmol/L Tris-HCl buffer, pH 7.50. Cell disruption was performed using ultrasonic treatment (Sonoplus HD 3200, Bandelin, Germany) in two cycles of 9 min each at 50% amplitude, at a cell concentration of γ_{cells} = 15 mg/mL. An ice bath was used through sonication to minimize heating and prevent enzyme denaturation. Following sonication, the lysate was centrifuged for 45 min at 14,000 rpm and T = 4 °C (Universal 320 R, Hettich Zentrifugen, Kirchlengern, Germany). Cell debris was removed, and the crude enzyme was recovered in the supernatant.

3.2.10. Purification of Recombinant [NiFe]-Hydrogenase from *E. coli* BL21 (DE3)

Frozen *E. coli* BL21 (DE3) cells expressing recombinant [NiFe]-hydrogenase were thawed and weighed (~2 g) after 4 mL of lysis buffer was added. The contents were carefully resuspended in the buffer (50 mmol/L Tris-HCl buffer, pH 7.50) and placed on ice. Cells were disrupted by sonication in two cycles of 5 min at 80% amplitude with a 2 s pulse interval. After sonication, cell debris was removed by centrifugation for 45 min at 15,000 rpm and T = 4 °C. The lysate was filtered through a 0.45 µm pore size filter (Chromafil Xtra RC-45/25 0.45 µm, Macherey-Nagel, Düren, Germany). Recombinant [NiFe]-hydrogenase was purified using a StrepTrap XT column, following the procedure described by Lauterbach et al. [32], with the modification that the entire process was performed under aerobic conditions. Purified SH was used immediately for activity assays. For short-term storage, samples were kept on ice at T = 4 °C and used within 2–3 h; freezing was not applied. Enzyme activity and protein concentration in the eluate were determined spectrophotometrically using the assays described in Sections 3.2.3 and 3.2.5, respectively.

3.2.11. NAD(P)H Oxidation in a Batch Reactor

NAD(P)H oxidation experiments were carried out in a batch reactor (V = 50 mL) at pH 7.00 and T = 35 °C for to 30 min under constant stirring with a magnetic stirrer (Thermomix 1420, Braun, Germany). The reaction mixture contained 50 mmol/L Tris-HCl buffer, pH 7.00, and 0.2 mmol/L NAD(P)H. The reaction was initiated by the addition of either crude extract (γ = 0.0371 mg/mL) or purified enzyme (γ = 0.0119 mg/mL). Samples were taken from the reaction mixture at defined time intervals and filtered (Chromafil Xtra PA-20/25; 0.2 µm, 25 mm, Macherey-Nagel, Düren, Germany) to stop the reaction. The NAD(P)H concentration was determined spectrophotometrically, and the amount of $NAD(P)^+$ produced was calculated from the NAD(P)H consumption using the stoichiometric ratio. All measurements fall within a confidence interval of ±0.05.

3.2.12. Glucose Oxidation and Coenzyme Regeneration in a Batch Reactor

Glucose oxidation catalysed by GDH and parallel coenzyme regeneration by [NiFe]-hydrogenase were carried out in a batch reactor (V = 100 mL). The coenzyme was regenerated using either crude or purified enzyme. Reaction mixtures contained glucose ($c_{glucose}$ = 2 mmol/L), NAD^+ (c_{NAD+} = 5 mmol/L), GDH (γ_{GDH} = 0.003 mg/mL), hydrogenase (γ_{Hyd} = 0.0069 mg/mL), and 20 mmol/L Tris-HCl buffer (pH 7.0). Reactions were performed at T = 35 °C under aerobic conditions. Glucose consumption and NADH formation were monitored spectrophotometrically. All measurements fall within a confidence interval of ±0.05.

4. Conclusions

This study demonstrates that recombinant expression of the soluble [NiFe]-hydrogenase from *C. necator* H16 in *E. coli* BL21 (DE3) yields an active and function-

ally competent biocatalyst capable of catalysing NAD^+/NADH interconversion. The enzyme was successfully produced, released by ultrasonic lysis, partially characterized in crude form, and subsequently purified. SDS-PAGE analysis confirmed the presence of all expected structural subunits. Activity profiling revealed defined pH optima, and a temperature optimum of 35 °C, consistent with the behaviour reported for other soluble [NiFe]-hydrogenases. Stability studies further highlighted the enzyme's sensitivity to elevated temperatures, reinforcing the importance of low-temperature handling for maintaining catalytic integrity. Coenzyme stability experiments provided essential insight for the design of efficient regeneration systems. Both NADH and NADPH were highly stable under neutral conditions but underwent rapid degradation under acidic conditions. Batch reactor experiments confirmed that the recombinant hydrogenase is highly specific towards NADH, with significantly lower activity towards NADPH. Moreover, crude extracts from recombinant *E. coli* displayed higher apparent coenzyme regeneration than the purified enzyme. This enhancement is likely due to the presence of additional endogenous enzymes, such as NADH oxidase, and stabilising cellular components. In contrast, crude extract from wild-type *C. necator* H16 showed markedly lower activity, reflecting the advantage of heterologous overexpression systems for producing catalytically active hydrogenase.

Coupling the hydrogenase with GDH demonstrated that the enzyme is, in principle, capable of sustaining NAD^+ regeneration within a multi-enzymatic cascade. However, the reaction rapidly ceased due to the accumulation of gluconic acid and the resulting sharp pH decrease. This pH shift simultaneously inactivated both GDH and the hydrogenase and accelerated NADH degradation. Consequently, the primary limitation in the current system is not the intrinsic catalytic capacity of the hydrogenase but the instability of the reaction environment. These results clearly show that effective pH control is essential for enabling continuous and efficient cofactor regeneration.

Overall, this work establishes a solid functional basis for the application of recombinant soluble [NiFe]-hydrogenase in NAD^+ regeneration systems. It also highlights key engineering priorities for the future, including pH stabilisation, protection of coenzyme integrity, and optimisation of reaction conditions. Addressing these challenges will be crucial for advancing hydrogenase-driven bioprocesses and biohydrogen production technologies. A promising strategy to overcome current limitations is the transition from batch to continuous operation.

Author Contributions: Conceptualization, R.V. and A.Š.; methodology, A.Š.; software, R.V. and A.J.T.; formal analysis, R.V., M.M. and Z.K.; investigation, R.V., M.M. and Z.K.; data curation, R.V. and A.Š.; writing—original draft preparation, R.V.; writing—review and editing, Z.K., A.Š., A.J.T. and B.Z.; visualization, A.Š.; supervision, B.Z.; project administration, B.Z.; funding acquisition, B.Z. All authors have read and agreed to the published version of the manuscript.

Funding: This research was funded by Croatian Science Foundation (HrZZ), grant number IP-2022-10-2175 and DOK-NPOO-2023-10-3890.

Data Availability Statement: Data will be available on request.

Conflicts of Interest: The authors declare no conflicts of interest.

Appendix A

Table A1. Experimental design of crude [NiFe]-hydrogenase extraction according to the Box-Behnken experimental design.

Exp.	t (min)	A (%)	γ (mg/mL)	V.A. (U/mL)
1	3	40	10	0.130 ± 0.007

Table A1. *Cont.*

Exp.	*t* (min)	*A* (%)	γ (mg/mL)	V.A. (U/mL)
2	3	60	10	0.180 ± 0.015
3	9	40	10	0.225 ± 0.018
4	9	60	10	0.118 ± 0.019
5	6	40	5	0.122 ± 0.013
6	6	60	5	0.091 ± 0.021
7	6	40	15	0.234 ± 0.097
8	6	60	15	0.144 ± 0.024
9	3	50	5	0.089 ± 0.024
10	9	50	5	0.148 ± 0.001
11	3	50	15	0.246 ± 0.079
12	9	50	15	0.300 ± 0.022
13	6	50	10	0.232 ± 0.017
14	6	50	10	0.275 ± 0.028
15	6	50	10	0.236 ± 0.001
16	6	50	10	0.250 ± 0.075
17	6	50	10	0.202 ± 0.020

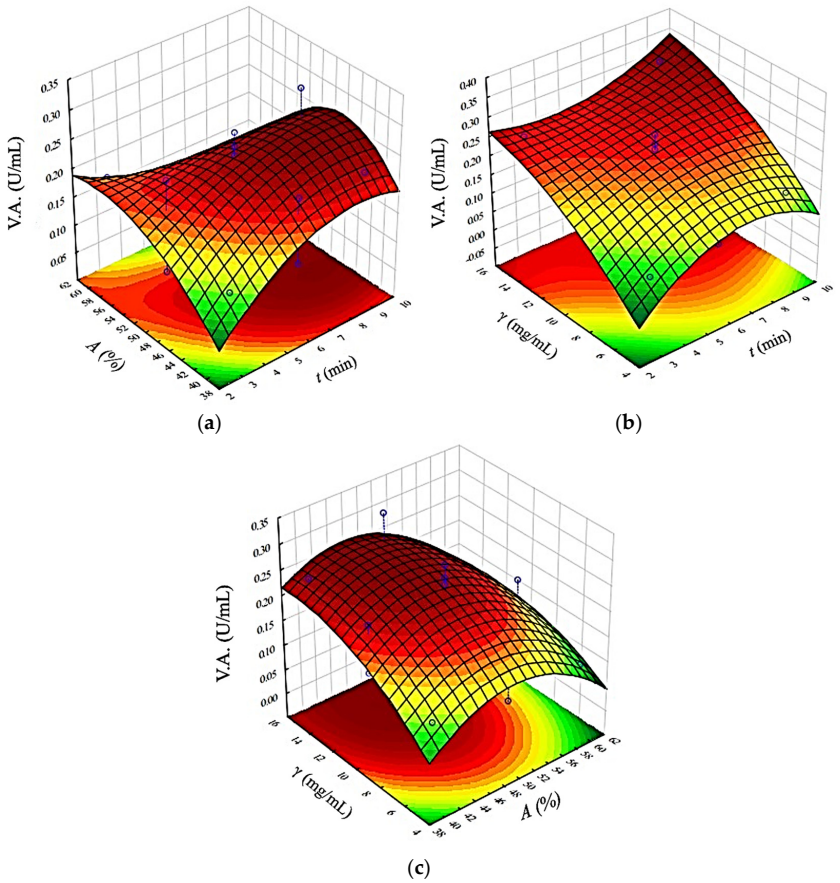

Figure A1. 3D representation of the influence of ultrasonic treatment conditions on the volumetric activity of crude [NiFe]-hydrogenase: (**a**) time of disruption and amplitude, (**b**) cell concentration and amplitude and (**c**) cell concentration and time of disruption.

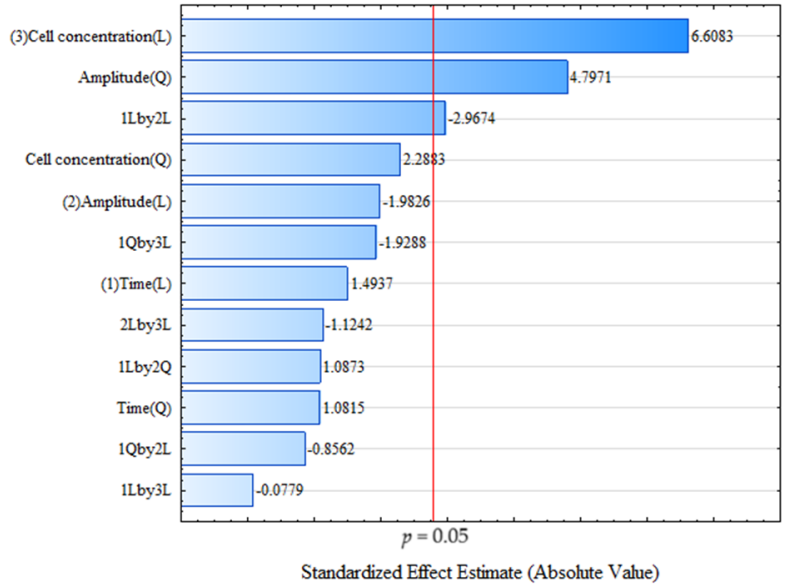

Figure A2. Pareto diagram showing the standardized effect estimates (absolute values) of the main factors and their interactions on the response variable. Factors include disruption time (1), ultrasound amplitude (2), and cell concentration (3), with linear (L) and quadratic (Q) terms. The red vertical line represents the threshold for statistical significance at $p = 0.05$.

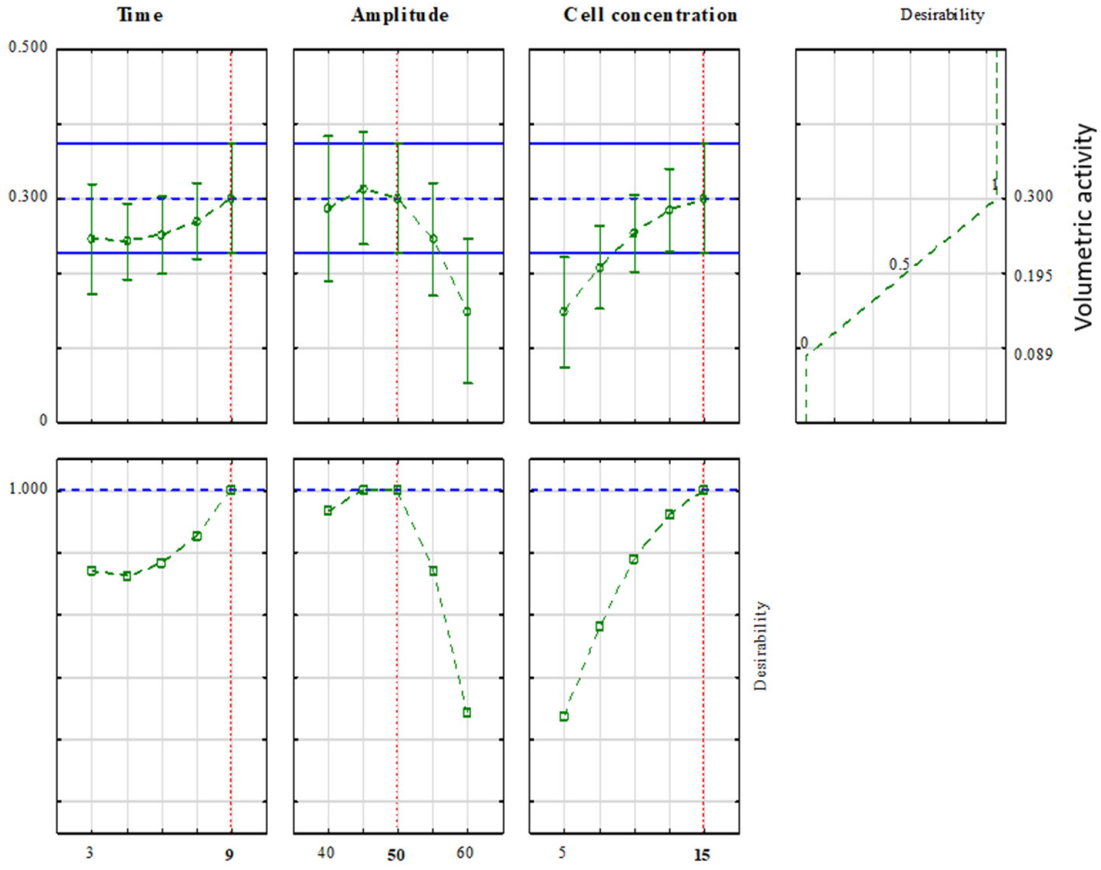

Figure A3. Predicted value profiles and desirability functions for the determination of the optimal ultrasonic treatment conditions $t = 9$ min, $A = 50\%$ and $\gamma = 15$ mg/mL.

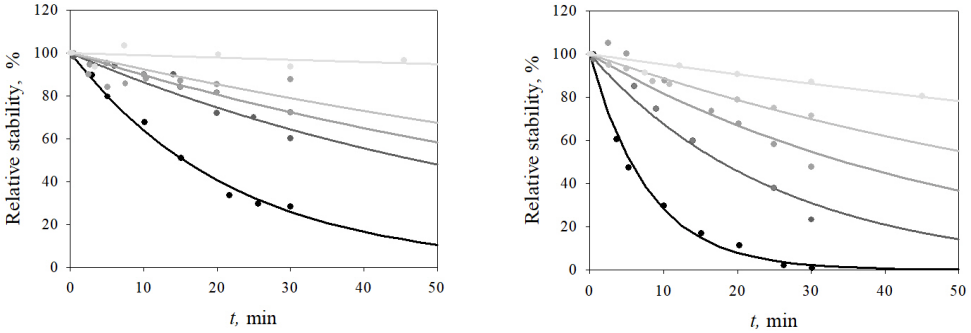

Figure A4. Stability of the coenzymes (**a**) NADH and (**b**) NADPH at different pH values (● pH = 4.25, ● pH = 4.50, ● pH = 5.00, ● pH = 6.00, ● pH = 7.00, – mathematical model) at T = 35 °C.

Table A2. Comparison of the degradation constants for the coenzymes NADH and NADPH at different pH values.

pH	Coenzyme	
	NADH	NADPH
	k (1/min)	k (1/min)
4.25	0.0449 ± 0.0014	0.1268 ± 0.0060
4.60	0.0147 ± 0.0013	0.0390 ± 0.0025
5.00	0.0108 ± 0.0003	0.0200 ± 0.0020
6.00	0.0079 ± 0.0020	0.0119 ± 0.0005
7.00	0.0011 ± 0.0006	0.0049 ± 0.0004

References

1. Leone, L.; Sgueglia, G.; La Gatta, S.; Chino, M.; Nastri, F.; Lombardi, A. Enzymatic and Bioinspired Systems for Hydrogen Production. *Int. J. Mol. Sci.* **2023**, *24*, 8605. [CrossRef]
2. Boyd, E.S.; Colman, D.R.; Templeton, A.S. Perspective: Microbial hydrogen metabolism in rock-hosted ecosystems. *Front. Energy. Res.* **2024**, *12*, 1340410. [CrossRef]
3. Schiffels, J.; Pinkenburg, O.; Schelden, M.; Aboulnaga, E.-H.A.A.; Baumann, M.E.M.; Selmer, T. An Innovative Cloning Platform Enables Large-Scale Production and Maturation of an Oxygen-Tolerant [NiFe]-Hydrogenase from *Cupriavidus necator* in *Escherichia coli*. *PLoS ONE* **2013**, *8*, e68812. [CrossRef]
4. Al-Shameri, A.; Petrich, M.C.; Puring, K.J.; Apfel, U.P.; Nestl, B.M.; Lauterbach, L. Powering artificial enzymatic cascades with electrical energy. *Angew. Chem. Int. Ed.* **2020**, *59*, 10929–10933. [CrossRef] [PubMed]
5. Al-Shameri, A.; Borlinghaus, N.; Weinmann, L.; Scheller, P.N.; Nestl, B.M.; Lauterbach, L. Synthesis of N-heterocycles from diamines via H_2-driven NADPH recycling in the presence of O_2. *Green Chem.* **2019**, *21*, 1463–9262. [CrossRef]
6. Lauterbach, L.; Lenz, O. How to make the reducing power of H_2 available for in vivo biosyntheses and biotransformations. *Curr. Opin. Chem. Biol.* **2019**, *49*, 91–96. [CrossRef] [PubMed]
7. Al-Shameri, A.; Siebert, D.L.; Sutiono, S.; Lauterback, L.; Sieber, V. Hydrogenase-based oxidative biocatalysis without oxygen. *Nat. Commun.* **2023**, *14*, 2693. [CrossRef]
8. Wulff, P.; Thomas, C.; Sargent, F.; Armstrong, F.A. How the oxygen tolerance of a [NiFe]-hydrogenase depends on quaternary structure. *J. Biol. Inorg. Chem.* **2016**, *21*, 121–134. [CrossRef]
9. Sim, M.S.; Park, S.H.; Choi, J.I.; Kim, T.W. Development of a highly efficient microbial fermentation process of recombinant *Escherichia coli* for GABA production from glucose. *J. Biotech.* **2025**, *399*, 72–80. [CrossRef]
10. Ojima, Y.; Saito, H.; Miyuki, S.; Fukunaga, K.; Tsuboi, T.; Azuma, M. Induction conditions that promote the effect of glycerol on recombinant protein production in *Escherichia coli*. *Biotechnol. Rep.* **2025**, *46*, e00898. [CrossRef]
11. Kim, J.Y.H.; Jo, B.H.; Cha, H.J. Production of biohydrogen by recombinant expression of [NiFe]-hydrogenase 1 in *Escherichia coli*. *Microb. Cell Fact.* **2010**, *9*, 54. [CrossRef]
12. Kim, J.Y.H.; Jo, B.H.; Cha, H.J. Production of biohydrogen by heterologous expression of oxygen-tolerant *Hydrogenovibrio marinus* [NiFe]-hydrogenase in *Escherichia coli*. *J. Biotech.* **2011**, *155*, 312–315. [CrossRef]
13. Du, F.; Liu, Y.Q.; Xu, Y.S.; Li, Z.J.; Wang, Y.Z.; Zhang, Z.X.; Sun, X.M. Regulating the T7 RNA polymerase expression in *E. coli* BL21 (DE3) to provide more host options for recombinant protein production. *Microb. Cell Factories* **2021**, *20*, 189. [CrossRef] [PubMed]

14. Fan, Q.; Neubauer, P.; Lenz, O.; Gimpel, M. Heterologous Hydrogenase Overproduction Systems for Biotechnology—An Overview. *Int. J. Mol. Sci.* **2020**, *21*, 5890. [CrossRef] [PubMed]
15. Lacasse, M.J.; Zamble, D.B. [NiFe]-Hydrogenase Maturation. *Biochemistry* **2016**, *55*, 1689–1701. [CrossRef]
16. Böck, A.; King, P.W.; Blokesch, M.; Posewitz, M.C. Maturation of Hydrogenases. *Adv. Microb. Physiol.* **2006**, *51*, 1–71. [CrossRef] [PubMed]
17. Noor, N.D.M.; Nishikawa, K.; Nishihara, H.; Yoon, K.S.; Ogo, S.; Higuchi, Y. Improved purification, crystallization and crystallographic study of Hyd-2-type [NiFe]-hydrogenase from Citrobacter sp. S-77. *Acta Crystallogr. Sect. F* **2016**, *72*, 53–58. [CrossRef]
18. Al-saari, N.; Amada, E.; Matsumura, Y.; Tanaka, M.; Mino, S.; Sawabe, T. Understanding the NaCl-dependent behavior of hydrogen production of a marine bacterium, *Vibrio tritonius*. *PeerJ* **2019**, *7*, e6769. [CrossRef]
19. Tremblay, P.L.; Lovley, D.R. Role of the NiFe hydrogenase Hya in oxidative stress defense in Geobacter sulfurreducens. *J. Bacteriol.* **2012**, *194*, 2248–2253. [CrossRef]
20. Romig, M.; Eberwein, M.; Deobald, D.; Schmid, A. Reactivation and long-term stabilization of the [NiFe] Hox hydrogenase of *Synechocystis* sp. PCC6803 by glutathione after oxygen exposure. *J. Biol. Chem.* **2025**, *301*, 108086. [CrossRef]
21. Ruff, A.; Szczesny, J.; Zacarias, S.; Pereira, I.A.C.; Plumeré, N.; Schuhmann, W. Protection and Reactivation of the [NiFeSe] Hydrogenase from *Desulfovibrio vulgaris* Hildenborough under Oxidative Conditions. *ACS Energy Lett.* **2017**, *2*, 964–968. [CrossRef]
22. Lamont, C.M.; Sargent, F. Design and characterisation of synthetic operons for biohydrogen technology. *Arch. Microbiol.* **2017**, *199*, 495–503. [CrossRef] [PubMed]
23. Šalić, A.; Zelić, B. A Game Changer: Microfluidic Technology for Enhancing Biohydrogen Production—Small Size for Great Performance. *Energies* **2022**, *15*, 7065. [CrossRef]
24. Martínez, A.T.; Ruiz-Dueñas, F.J.; Camarero, S.; Serrano, A.; Linde, D.; Lund, H.; Vind, J.; Tovborg, M.; Herold-Majumdar, O.M.; Hofrichter, M.; et al. Oxidoreductases on their way to industrial biotransformations. *Biotechnol. Adv.* **2017**, *35*, 815–831. [CrossRef]
25. Nowak, C.; Beer, B.; Pick, A.; Roth, T.; Lommes, P.; Sieber, V.A. water-forming NADH oxidase from *Lactobacillus pentosus* suitable for the regeneration of synthetic biomimetic cofactors. *Front. Microbiol.* **2015**, *6*, 957. [CrossRef]
26. Kumar, P.; Pai, K.; Pandey, H.P.; Sundar, S. NADH-oxidase, NADPH-oxidase and myeloperoxidase activity of visceral leishmaniasis patients. *J. Med. Microbiol.* **2002**, *51*, 832–836. [CrossRef]
27. Riebel, B.R.; Gibbs, P.R.; Wellborn, W.B.; Bommarius, A.S. Cofactor regeneration of NAD^+ from NADH: Novel water-forming NADH oxidases. *Adv. Synth. Catal.* **2002**, *344*, 1156–1168. [CrossRef]
28. Al-Shameri, A.; Schmermund, L.; Sieber, V. Engineering approaches for O_2-dependent enzymes. *Curr. Opin. Green Sustain. Chem.* **2023**, *40*, 100733. [CrossRef]
29. Xing, W.; Xing, W.; Yin, M.; Lv, Q.; Hu, Y.; Liu, C.; Zhang, J. Oxygen solubility, diffusion coefficient, and solution viscosity. In *Rotating Electrodemethods and Oxygen Reduction Electrocatalysts*; Xing, W., Yin, G., Zhang, J., Eds.; Elsevier: Amsterdam, The Netherlands, 2014; pp. 1–33. [CrossRef]
30. Ratzka, J.; Lauterbach, L.; Lenz, O.; Ansorge-Schumacher, M.B. Systematic evaluation of the dihydrogen-oxidising and NAD^+-reducing soluble [Nife]-hydrogenase from *Ralstonia Eutropha* H16 as a cofactor regeneration catalyst. *Biocatal. Biotransform.* **2011**, *29*, 246–252. [CrossRef]
31. Al-Shameri, A.; Willot, S.J.P.; Paul, C.E.; Hollmann, F.; Lauterbach, L. H_2 as a fuel for flavin- and H_2O_2-dependent biocatalytic reactions. *Chem. Commun.* **2020**, *56*, 9667–9670. [CrossRef]
32. Lauterbach, L.; Lenz, O. Catalytic production of hydrogen peroxide and water by oxygen-tolerant [NiFe]-hydrogenase during H_2 cycling in the presence of O_2. *J. Am. Chem. Soc.* **2013**, *135*, 17897–17905. [CrossRef]
33. Vincent, K.A.; Parkin, A.; Armstrong, F.A. Investigating and Exploiting the Electrocatalytic Properties of Hydrogenases. *Chem. Rev.* **2007**, *107*, 4366–4413. [CrossRef]
34. Sokolova, D.; Vincent, K.A. Exploiting hydrogenases for biocatalytic hydrogenations. *Chem. Commun.* **2024**, *60*, 13667–13677. [CrossRef] [PubMed]
35. Greening, C.; Kropp, A.; Vincent, K.; Grinter, R. Developing high-affinity, oxygen-insensitive [NiFe]-hydrogenases as biocatalysts for energy conversion. *Biochem. Soc. Trans.* **2023**, *51*, 1921–1933. [CrossRef] [PubMed]
36. Evans, R.M.; Beaton, S.E.; Rodriguez Macia, P.; Pang, Y.; Long Wong, K.; Kertess, L.; Myers, W.K.; Bjornsson, R.; Ash, P.A.; Vincent, K.A.; et al. Comprehensive structural, infrared spectroscopic and kinetic investigations of the roles of the active-site arginine in bidirectional hydrogen activation by the [NiFe]-hydrogenase 'Hyd-2' from *Escherichia coli*. *Chem. Sci.* **2023**, *14*, 8531–8551. [CrossRef]
37. Reeve, H.A.; Nicholson, J.; Altaf, F.; Lonsdale, T.H.; Preissler, J.; Lauterbach, L.; Lenz, O.; Leimkühler, S.; Hollmann, F.; Paul, C.E.; et al. A hydrogen-driven biocatalytic approach to recycling synthetic analogues of NAD(P)H. *Chem. Commun.* **2022**, *58*, 10540–10543. [CrossRef] [PubMed]
38. Ludwig, M.; Cracknell, J.A.; Vincent, K.A.; Armstrong, F.A.; Lenz, O. Oxygen-tolerant H2 oxidation by membrane-bound [NiFe] hydrogenases of ralstonia species. Coping with low level H2 in air. *J. Biol. Chem.* **2009**, *284*, 465–477. [CrossRef]

39. Feliu, J.X.; Cubarsi, R.; Villaverde, A. Optimized release of recombinant proteins by ultrasonication of *E. coli* cells. *Biotechnol. Bioeng.* **1998**, *58*, 536–540. [CrossRef]
40. Fan, Q.; Caserta, G.; Lorent, C.; Zebger, I.; Neubauer, P.; Lenz, O.; Gimpel, M. High-Yield Production of Catalytically Active Regulatory [NiFe]-Hydrogenase from *Cupriavidus necator* in *Escherichia coli*. *Front. Microbiol.* **2022**, *13*, 894375. [CrossRef]
41. Alfano, M.; Cavazza, C. Structure, function, and biosynthesis of nickel-dependent enzymes. *Protein. Sci.* **2020**, *29*, 1071–1089. [CrossRef]
42. Claire, M. Investigating the Impact of Temperature and pH on Enzyme Activity: A Kinetic Analysis. *Biochem. Physiol.* **2025**, *14*, 508.
43. Gu, Y. The effect of buffer pH on enzyme activity. *TNS* **2024**, *33*, 137–147. [CrossRef]
44. Peterson, M.E.; Daniel, R.M.; Danson, M.J.; Eisental, R. The dependence of enzyme activity on temperature: Determination and validation of parameters. *Biochem. J.* **2007**, *402*, 331–337. [CrossRef]
45. Wojcik, M.; Milek, J. A new method to determine optimum temperature and activation energies for enzymatic reactions. *Bioprocess. Biosyst. Eng.* **2016**, *39*, 1319–1323. [CrossRef]
46. Yagi, T.; Higuchi, Y. Studies on hydrogenase. *Proc. Jpn. QAQcad Ser. B Phys. Biol. Sci.* **2013**, *89*, 16–33. [CrossRef] [PubMed]
47. Hardt, S.; Stapf, S.; Filmon, D.; Birrel, J.A.; Rudiger, O.; Fourmond, V.; Leger, C.; Plumere, N. Reversible H_2 Oxidation and Evolution by Hydrogenase Embedded in a Redox Polymer Film. *Nat. Catal.* **2021**, *4*, 251–258. [CrossRef] [PubMed]
48. Alberty, R.A. Changes in binding of hydrogen ions in enzyme-catalyzed reactions. *Biophys. Chem.* **2007**, *125*, 328–333. [CrossRef]
49. Wolfe, K.D.; Alahuhta, M.; Himmel, M.E.; Bomble, Y.J.; Jennings, G.K.; Cliffel, D.E. Long-Term Stability of Nicotinamide Cofactors in Common Aqueous Buffers: Implications for Cell-Free Biocatalysis. *Molecules* **2024**, *29*, 5453. [CrossRef] [PubMed]
50. Tsygankov, A.A.; Minakov, E.A.; Zorin, N.A.; Karyakin, A.A. Measuring the pH dependence of hydrogenase activities. *Biochemistry* **2007**, *72*, 968–973. [CrossRef]
51. Schmitz, O.; Boison, G.; Salzmann, H.; Bothe, H.; Schütz, K.; Wang, S.; Happe, T. HoxE—A subunit specific for the pentameric bidirectional hydrogenase complex (HoxEFUYH) of cyanobacteria. *Biochim. Biophys. Acta (BBA) - Bioenerg.* **2002**, *1554*, 66–74. [CrossRef]
52. Ma, K.; Schicho, R.N.; Kelly, R.M.; Adams, M.W. Hydrogenase of the hyperthermophile *Pyrococcus furiosus* is an elemental sulfur reductase or sulfhydrogenase: Evidence for a sulfur-reducing hydrogenase ancestor. *Proc. Natl. Acad. Sci. USA* **1993**, *90*, 5341–5344. [CrossRef]
53. Flanagan, L.A.; Wright, J.J.; Roessler, M.M.; Moir, J.W.; Parkin, A. Re-engineering a NiFe hydrogenase to increase the H_2 production bias while maintaining native levels of O_2 tolerance. *Chem. Commun.* **2016**, *52*, 9133–9136. [CrossRef]
54. Lu, Y.; Koo, J. O_2 sensitivity and H_2 production activity of hydrogenases—A review. *Biotechnol. Bioeng.* **2019**, *116*, 3124–3135. [CrossRef] [PubMed]
55. Preissler, J.; Wahlefeld, S.; Lorent, C.; Teutloff, C.; Horch, M.; Lauterbach, L.; Cramer, S.P.; Zebger, I.; Lenz, O. Enzymatic and spectroscopic properties of a thermostable [NiFe]-hydrogenase performing H_2-driven NAD^+-reduction in the presence of O_2. *Biochim. Biophys. Acta Bioenerg.* **2018**, *1859*, 8–18. [CrossRef]
56. Yonemoto, I.T.; Matteri, C.W.; Nguyen, T.A.; Smith, H.O.; Weyman, P.D. Dual organism design cycle reveals small subunit substitutions that improve [NiFe] hydrogenase hydrogen evolution. *J. Biol. Eng.* **2013**, *7*, 17. [CrossRef]
57. Arcus, V.L.; Prentice, E.J.; Hobbs, J.K.; Mulholland, A.J.; Van der Kamp, M.W.; Pudney, C.R.; Parker, E.J.; Schipper, L.A. On the Temperature Dependence of Enzyme-Catalyzed Rates. *Biochemistry* **2016**, *55*, 1681–1688. [CrossRef] [PubMed]
58. Chowdhury, S.P.; Conrad, R. Thermal deactivation of high-affinity H_2 uptake activity in soils. *Soil. Biol. Biochem.* **2010**, *42*, 1574–1580. [CrossRef]
59. Keefe, R.G.; Axley, M.J.; Harabin, A.L. Kinetic Mechanism Studies of the Soluble Hydrogenase from *Alcaligenes eutrophus* H16. *Arch. Biochem. Biophys.* **1995**, *317*, 449–456. [CrossRef] [PubMed]
60. Robinson, P.K. Enzymes: Principles and biotechnological applications. *Essays Biochem.* **2015**, *59*, 1–41. [CrossRef]
61. Scopes, R.K. *Protein Purification*; Springer: New York, NY, USA, 2013.
62. Watthanasakphuban, N.; Srila, P.; Pinmanee, P.; Pinmanee, P.; Punvittayagul, C.; Petchyam, N.; Ninchan, B. Production, purification, characterization, and safety evaluation of constructed recombinant D-psicose 3-epimerase. *Microb. Cell Factories* **2024**, *23*, 216. [CrossRef]
63. Smith, B.J. SDS Polyacrylamide Gel Electrophoresis of Proteins. *Methods Mol. Biol.* **1984**, *1*, 41–55. [CrossRef] [PubMed]
64. da Costa Silva, M.; Bezzera Costa, R.; Oliveira dos Santos Gomes, M.M.; Santos do Nascimento, J.; da Silva Gonçalves, A.H.; Alves Nunes, J.; Angelo dos Santos, M.; Soares Gomes, F.; Rodrigues da Luz, J.M.; Meireles Grillo, L.A. Purification and Functional Characterization of a New Endoglucanase from *Pleurotus djamor* PLO13 Produced by Solid-State Fermentation of Agro-Industrial Waste. *Fermentation* **2025**, *11*, 182. [CrossRef]
65. Burgdorf, T.; van der Linden, E.; Bernhard, M.; Yin, Q.Y.; Back, J.W.; Hartog, A.F.; Muijsers, A.O.; de Koster, C.G.; Albracht, S.P.; Friedrich, B. The soluble NAD^+-Reducing [NiFe]-hydrogenase from *Ralstonia eutropha* H16 consists of six subunits and can be specifically activated by NADPH. *J. Bacteriol.* **2005**, *187*, 3122–3132. [CrossRef] [PubMed]

66. Burgdorf, T.; Lenz, O.; Buhrke, T.; Linden, E.; Jones, A.; Albracht, S.; Friedrich, B. [NiFe]-Hydrogenases of *Ralstonia eutropha* H16: Modular Enzymes for Oxygen-Tolerant Biological Hydrogen Oxidation. *J. Mol. Microbiol. Biotechnol.* **2005**, *10*, 181–196. [CrossRef] [PubMed]
67. Lauterbach, L.; Idris, Z.; Vincent, K.A.; Lenz, O. Catalytic Properties of the Isolated Diaphorase Fragment of the NAD^+-Reducing [NiFe]-Hydrogenase from *Ralstonia eutropha*. *PLoS ONE* **2011**, *6*, e25939. [CrossRef]
68. Hummel, W.; Riebel, B. Isolation and biochemical characterization of a new NADH oxidase from *Lactobacillus brevis*. *Biotechnol. Lett.* **2003**, *25*, 51–54. [CrossRef]
69. Nishiyama, Y.; Massey, V.; Takeda, K.; Kawasaki, S.; Sato, J.; Watanabe, T.; Niimura, Y. Hydrogen peroxide-forming NADH oxidase belonging to the peroxiredoxin oxidoreductase family: Existence and physiological role in bacteria. *J. Bacteriol.* **2001**, *183*, 2431–2438. [CrossRef]
70. Piszkiewicz, S.; Pielak, G.J. Protecting Enzymes from Stress-Induced Inactivation. *Biochem.* **2019**, *58*, 3825–3833. [CrossRef]
71. Dako, E.; Bernier, A.; Dadie, A.T.; Jankowski, C.K. *The Problems Associated with Enzyme Purification*, 1st ed.; Ekinci, D., Ed.; InTech: London, UK, 2012. [CrossRef]
72. Woodward, J.; Orr, M. Enzymatic conversion of sucrose to hydrogen. *Biotechnol. Prog.* **1998**, *14*, 897–902. [CrossRef]
73. Zhao, X.; Jiang, H.; Wang, S.; Yuan, X.; Feng, Y.; Yang, J.; Li, Y.; Zhu, N.; Zhao, S.; He, W.; et al. Microreactors in chemical process intensification: Chemical reactions, crystallizations, extractions and emulsifications. *Chem. Eng. J.* **2025**, *519*, 165223. [CrossRef]
74. Yang, Y.; Qian, J.; Fang, G.; Guan, Z.; Han, H.; Liu, Q.; Liu, H.; Wang, Y.; Li, W. Research progress on the process analysis technology for microreactors. *Microchem. J.* **2025**, *212*, 113373. [CrossRef]
75. Lane, T.G.; Revankar, S.T. Advances in technology, design and deployment of microreactors—A review. *Prog. Nucl. Energy* **2025**, *178*, 105520. [CrossRef]
76. da Silva, J.L., Jr.; Santana, H.S.; Hodapp, M.J. Microreactor technology applied to catalytic processing of Hydrogen: A review. *J. Ind. Eng. Chem.* **2025**, *143*, 65–84. [CrossRef]
77. Shaker, G.; Swift, C.J. *Peroxidase-Coupled Glucose Method*; StatPearls Publishing: Treasure Island, FL, USA, 2023. [PubMed]
78. Erst, O.; Zor, T. Linearization of the Bradford Assay. *J. Vis. Exp.* **2010**, *38*, 1918. [CrossRef]
79. Rover, L.J.; Fernandes, J.C.; de Oliviera Neto, G.; Kubota, L.T.; Katekawa, E.; Serrano, S.H. Study of NADH stability using ultraviolet-visible spectrophotometric analysis and factorial design. *Anal. Biochem.* **1998**, *260*, 50–55. [CrossRef] [PubMed]
80. Laemmli, U.K. Cleavage of structural proteins during the assembly of the head of bacteriophage T4. *Nature* **1970**, *227*, 680–695. [CrossRef]

Disclaimer/Publisher's Note: The statements, opinions and data contained in all publications are solely those of the individual author(s) and contributor(s) and not of MDPI and/or the editor(s). MDPI and/or the editor(s) disclaim responsibility for any injury to people or property resulting from any ideas, methods, instructions or products referred to in the content.